

UC San Diego

UC San Diego Previously Published Works

Title

Fluorescence-Guided Surgery of Liver Metastasis in Orthotopic Nude-Mouse Models

Permalink

<https://escholarship.org/uc/item/0nv0r7hz>

Journal

PLOS ONE, 10(10)

ISSN

1932-6203

Authors

Murakami, Takashi
Hiroshima, Yukihiro
Zhang, Yong
et al.

Publication Date

2015

DOI

10.1371/journal.pone.0138752

Copyright Information

This work is made available under the terms of a Creative Commons Attribution License, available at <https://creativecommons.org/licenses/by/4.0/>

Peer reviewed

RESEARCH ARTICLE

Fluorescence-Guided Surgery of Liver Metastasis in Orthotopic Nude-Mouse Models

Takashi Murakami^{1,2,3}, Yukihiro Hiroshima^{1,2,3}, Yong Zhang¹, Takashi Chishima³, Kuniya Tanaka³, Michael Bouvet², Itaru Endo³, Robert M. Hoffman^{1,2*}

1 AntiCancer, Inc., San Diego, California, United States of America, **2** Department of Surgery, University of California San Diego, San Diego, California, United States of America, **3** Department of Gastroenterological Surgery, Graduate School of Medicine, Yokohama City University, Yokohama, Japan

* all@anticancer.com



OPEN ACCESS

Citation: Murakami T, Hiroshima Y, Zhang Y, Chishima T, Tanaka K, Bouvet M, et al. (2015) Fluorescence-Guided Surgery of Liver Metastasis in Orthotopic Nude-Mouse Models. PLoS ONE 10(10): e0138752. doi:10.1371/journal.pone.0138752

Editor: Matthew Bogyo, Stanford University, UNITED STATES

Received: May 7, 2015

Accepted: September 3, 2015

Published: October 1, 2015

Copyright: © 2015 Murakami et al. This is an open access article distributed under the terms of the [Creative Commons Attribution License](https://creativecommons.org/licenses/by/4.0/), which permits unrestricted use, distribution, and reproduction in any medium, provided the original author and source are credited.

Data Availability Statement: All data underlying the findings in our study are freely available in the manuscript.

Funding: This study was supported by National Cancer Institute grant numbers CA132971 to MB and CA142669 to MB and JSPS KAKENHI grant numbers 26830081 to YH, 26462070 to IE and 24592009 to KT. The funders had no role in study design, data collection and analysis, decision to publish, or preparation of the manuscript. AntiCancer Inc. provided support in the form of salary for an author YZ, but did not have any additional role in the study design, data collection and analysis, decision to

Abstract

We report here the development of fluorescence-guided surgery of liver metastasis. HT29 human colon cancer cells expressing green fluorescent protein (GFP) were initially injected in the spleen of nude mice. Three weeks later, established liver metastases were harvested and implanted on the left lobe of the liver in other nude mice in order to make an orthotopic liver metastasis model. Fourteen mice with a single liver metastasis were randomized into bright-light surgery (BLS) or fluorescence-guided surgery (FGS) groups. Seven mice were treated with BLS, seven were treated with FGS. Three weeks after implantation, the left lobe of the liver with a single metastasis was exposed through a median abdominal incision. BLS was performed under white light. FGS was performed using a hand-held portable fluorescence imaging system (Dino-Lite). Post-surgical residual tumor fluorescence was visualized with the OV100 Small Animal Imaging System. Residual tumor fluorescence after BLS was clearly visualized at high magnification with the OV100. In contrast, residual tumor fluorescence after FGS was not detected even at high magnification with the OV100. These results demonstrate the feasibility of FGS for liver metastasis.

Introduction

The ability of the surgeon to accurately visualize tumor margins is essential at the time of surgery and is of particular importance for resection of metastatic disease, especially in the liver [1].

A variety of labeling compounds have been used for fluorescence-guided surgery in the clinic. Sentinel lymph nodes in breast cancer patients were labeled by a near-infrared (NIR) fluorescing dye indocyanine [2]. However, indocyanine does not specifically label tumor cells. The metabolite 5-aminolevulinic acid, a precursor of hemoglobin, labels porphyrins in malignant glioma for FGS [3], which significantly improved outcome.

Folate was coupled to fluorescein isothiocyanate (FITC) for targeting folate receptor- α (FR- α) in ovarian cancers. Under fluorescence-guided surgery, tumor deposits less than 1 mm in size could be visualized and resected [4].

Monoclonal antibodies directed against cancer antigen 19-9 (CA19-9) or carcino-embryonic antigen (CEA) were conjugated to a green fluorophore and delivered intravenously into

publish, or preparation of the manuscript. The specific roles of these authors are articulated in the 'author contributions' section.

Competing Interests: The authors have the following interests: Yong Zhang is an employee of AntiCancer Inc. Takashi Murakami and Robert M. Hoffman are unpaid affiliates of AntiCancer Inc. Yukihiro Hiroshima is a former unpaid affiliates of AntiCancer Inc. Robert M. Hoffman is a PLOS ONE Editorial Board Member. AntiCancer Inc. played an indirect role through the participation of the coauthors. There are no other competing interests. There are no patents, products in development or marketed products to declare. This does not alter the authors' adherence to all the PLOS ONE policies on sharing data and materials.

nude mice with orthotopic human pancreatic or colon tumors [5]. The tumors become fluorescent and were resected under fluorescence-guidance improved outcome [5–10].

Kishimoto *et al.* [11] labeled tumors with green fluorescence protein (GFP) using a telomerase-dependent adenovirus (OBP-401) that expresses the *gfp* gene only in cancer cells, which, in contrast to normal cells, express the telomerase enzyme. The labeled tumors could also be resected under fluorescence guidance. Tumors that recurred after fluorescence-guided surgery maintained GFP expression [12]. Since the cancer cells stably express GFP, detection of cancer recurrence and metastasis is possible with OBP-401 GFP labeling, and is not possible with nongenetic probes.

The present report demonstrates the feasibility of FGS of liver metastasis labeled with GFP in orthotopic mouse models.

Materials and Methods

Ethics Statement

All animal studies were conducted with an AntiCancer Institutional Animal Care and Use Committee (IACUC)-protocol specifically approved for this study and in accordance with the principals and procedures outlined in the National Institute of Health Guide for the Care and Use of Animals under Assurance Number A3873-1. In order to minimize any suffering of the animals, anesthesia and analgesics were used for all surgical experiments. Animals were anesthetized by intramuscular injection of a 0.02 ml solution of 20 mg/kg ketamine, 15.2 mg/kg xylazine, and 0.48 mg/kg acepromazine maleate. The response of animals during surgery was monitored to ensure adequate depth of anesthesia. Ibuprofen (7.5 mg/kg orally in drinking water every 24 hours for 7 days post-surgery) was used in order to provide analgesia post-operatively in the surgically-treated animals. The animals were observed on a daily basis and humanely sacrificed by CO₂ inhalation when they met the following humane endpoint criteria: prostration, skin lesions, significant body weight loss, difficulty breathing, epistaxis, rotational motion and body temperature drop. The use of animals was necessary to develop fluorescence-guided surgery of liver metastasis. Animals were housed with no more than 5 per cage. Animals were housed in a barrier facility on a high efficiency particulate arrestance (HEPA)-filtered rack under standard conditions of 12-hour light/dark cycles. The animals were fed an autoclaved laboratory rodent diet ([S1 ARRIVE Checklist](#)).

Cell Line

The human colon cancer cell line HT-29 [10], obtained from the American Type Culture Collection (Rockville, MD) was maintained in DMEM (Irvine Scientific, Irvine, CA) supplemented with heat-inactivated 10% fetal bovine serum (FBS) (Gemini Biologic Products, Calabasas, CA), 2 mM glutamine, 100 units/ml penicillin, 100 µg/ml streptomycin, and 0.25 µg/ml amphotericin B (Life Technologies, Inc., Grand Island, NY). The cells were incubated at 37°C in 5% CO₂.

Mice

Athymic *nu/nu* nude mice (AntiCancer Inc., San Diego, CA), 4–6 weeks old, were used in this study. Mice were kept in a barrier facility under HEPA filtration (as noted above). Mice were fed with an autoclaved laboratory rodent diet. All mouse surgical procedures and imaging were performed with the animals anesthetized by subcutaneous injection of the ketamine mixture described above. All animal studies were conducted with an AntiCancer Institutional Animal Care and Use Committee (IACUC)-protocol specifically approved for this study and in accordance with the principals and procedures outlined in the National Institute of Health Guide for the Care and Use of Animals under Assurance Number A3873-1.

Establishment of GFP-labeled HT29

For GFP gene transfection, 25% confluent HT-29 cells were incubated with a 1:1 mixture of GFP retroviral supernatants of PT67 packaging cells and RPMI 1640 cell culture medium (GIBCO Life Technologies, New York, NY) containing 10% FBS (Gemini Biological Products) for 72 h. Fresh medium was replenished at this time. Cells were harvested by trypsin-EDTA 72 h after transduction and subcultured at a ratio of 1:15 into medium, which contained 200 µg/ml G418 to select for high GFP expression, since the GFP retrovirus also contained the neomycin-resistance gene. The level of G418 was increased to 400 µg/ml stepwise. Clones stably expressing GFP were isolated with cloning cylinders (Bel-Art Products, Pequannock, NJ) with the use of trypsin-EDTA. The high-GFP-expressing cells were then amplified and transferred by conventional culture methods. High GFP-expression clones were then isolated in the absence of G418 for 10 passages to select for stable expression of GFP [13–15].

Initial Establishment of Liver Metastasis

HT-29-GFP cells were harvested by trypsinization and washed twice with serum-free medium. Cells (5×10^5 in 50 µl serum-free medium with 50% Matrigel) were injected into the superior

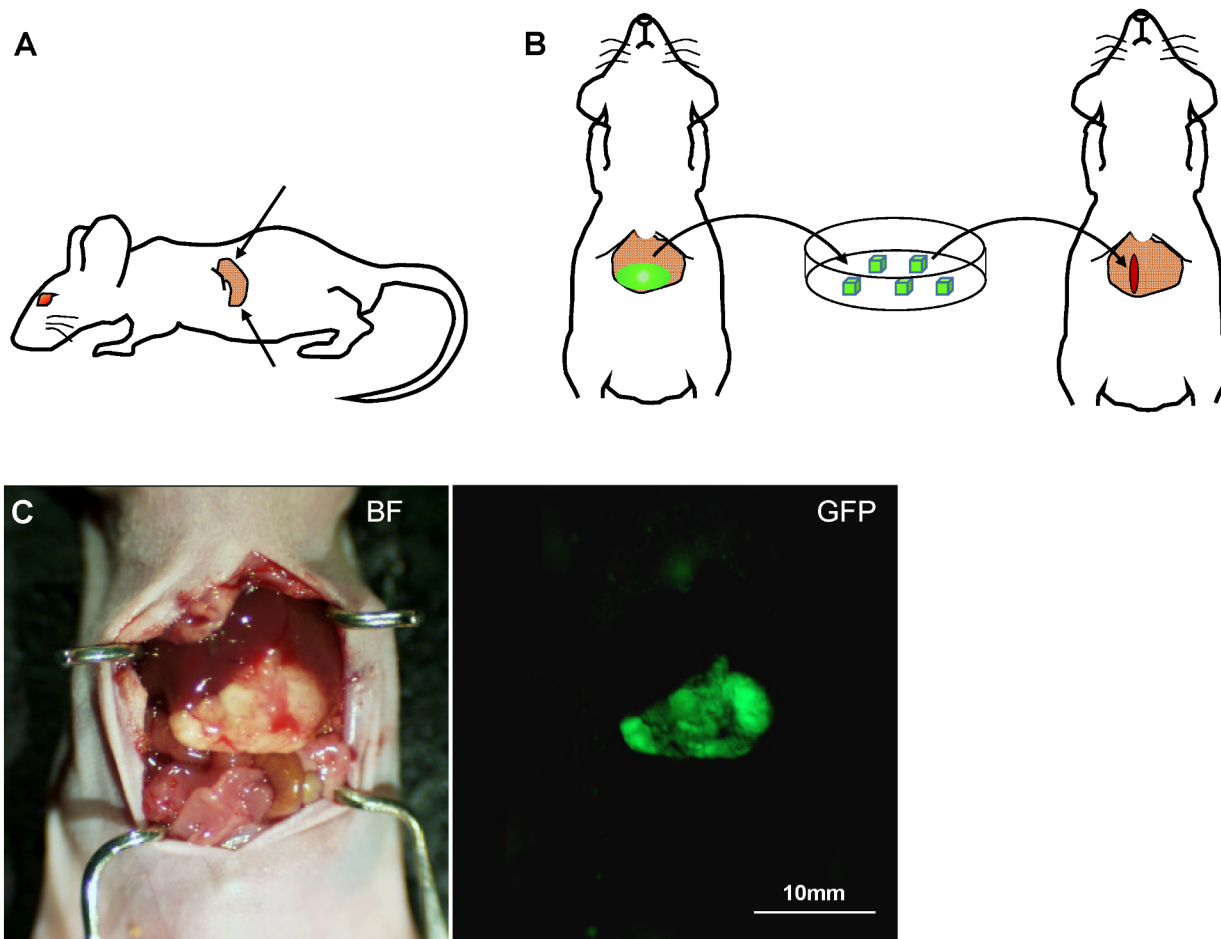


Fig 1. HT29-GFP colon cancer experimental liver metastasis. (A) HT-29-GFP cells (5×10^5 in 50 µl with 50% Matrigel) were injected into the superior pole and inferior pole of the spleen (arrows), respectively. (B) Three weeks after injection, liver metastasis was confirmed by laparotomy, which was resected and cut into 3-mm³ blocks. Each tumor fragment was implanted by surgical orthotopic implantation (SOI) in the left lobe of the liver on other nude mice. (C) Representative images of liver metastasis established after spleen injection. The large tumor in the liver strongly expressed GFP. (GFP, green fluorescent protein; BF, bright field)

doi:10.1371/journal.pone.0138752.g001

and inferior pole of the spleen in mice (Fig 1A). Three week after injection, liver metastasis was confirmed by laparotomy (Fig 1C).

Surgical orthotopic Implantation (SOI) of Liver Metastasis

Liver metastases were resected and cut into 8 mm³ blocks. A small 6- to 8-mm midline incision was made in other nude mice. The left lobe of the liver was exposed through this incision, and a single tumor fragment (3-mm³) was orthotopically implanted to the left lobe of the liver (Fig 1B). The left lobe of the liver was returned to the abdominal cavity, and the incision was closed in one layer using 6–0 nylon surgical sutures (Ethilon; Ethicon Inc., NJ, USA).

Bright-Light and Fluorescence-Guided Surgery of Liver Metastases

Four weeks after SOI of HT-29-GFP to the liver, the liver metastasis was exposed and imaged preoperatively with the OV100 Small Animal Imaging System (Olympus, Tokyo, Japan) [16] at a magnification of 0.14x. Fourteen mice underwent surgery: Fluorescence-guided surgery (FGS) in 7 mice and bright-light surgery (BLS) in 7 mice (Fig 2A and 2B). FGS was performed using the Dino-Lite imaging system (AM4113TGFBW Dino-Lite Premier; AnMo Electronics Corporation, New Taiwan). The surgical resection bed was imaged with the Olympus OV100 at a magnification of 0.14x or 0.56x to detect microscopic residual cancer. Residual tumor area was analyzed with ImageJ v1.49f (National Institutes of Health). The incision was closed in one layer using 6–0 nylon surgical sutures.

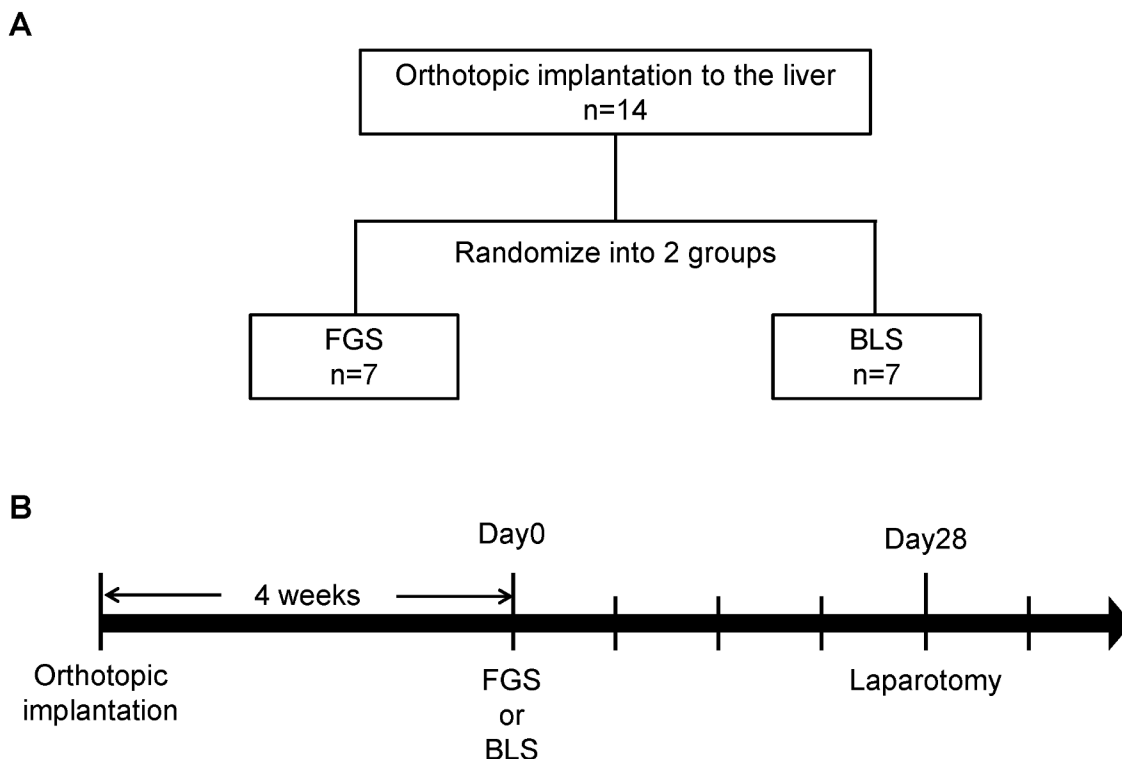


Fig 2. Schematic diagram of the experimental design. (A) Fourteen mice were randomized into 2 groups; FGS: n = 7, BLS: n = 7. (B) Timeline from orthotopic implantation. Four weeks after implantation, all mice were treated with FGS or BLS. Twenty-eight days after the surgery, all mice underwent laparotomy to detect GFP for evaluation of recurrence. After the laparotomy, follow-up examination for survival was continued. (FGS, fluorescence-guided surgery; BLS, bright-light surgery).

doi:10.1371/journal.pone.0138752.g002

Imaging of Tumor Progression

To evaluate tumor fluorescence around the resected site in the liver, laparotomy was performed in all mice at the 28th post-operative day (Fig 2B). Tumor fluorescence was detected with the OV100 and analyzed with ImageJ.

Tumor histology

Resected fresh tumor samples from either BLS or FGS were fixed in 10% formalin, and then embedded in paraffin. The tissue sections were deparaffinized in xylene and rehydrated in an ethanol series. Hematoxylin and eosin (H & E) staining was performed according to standard protocols. The margin between the tumor and the liver tissue was evaluated with a BHS System microscope (Olympus).

Statistical Analysis

SPSS statistics version 21.0 was used for all statistical analyses (IBM, New York City, NY, USA). Residual tumor area is expressed as mean \pm SD. Significant differences for continuous

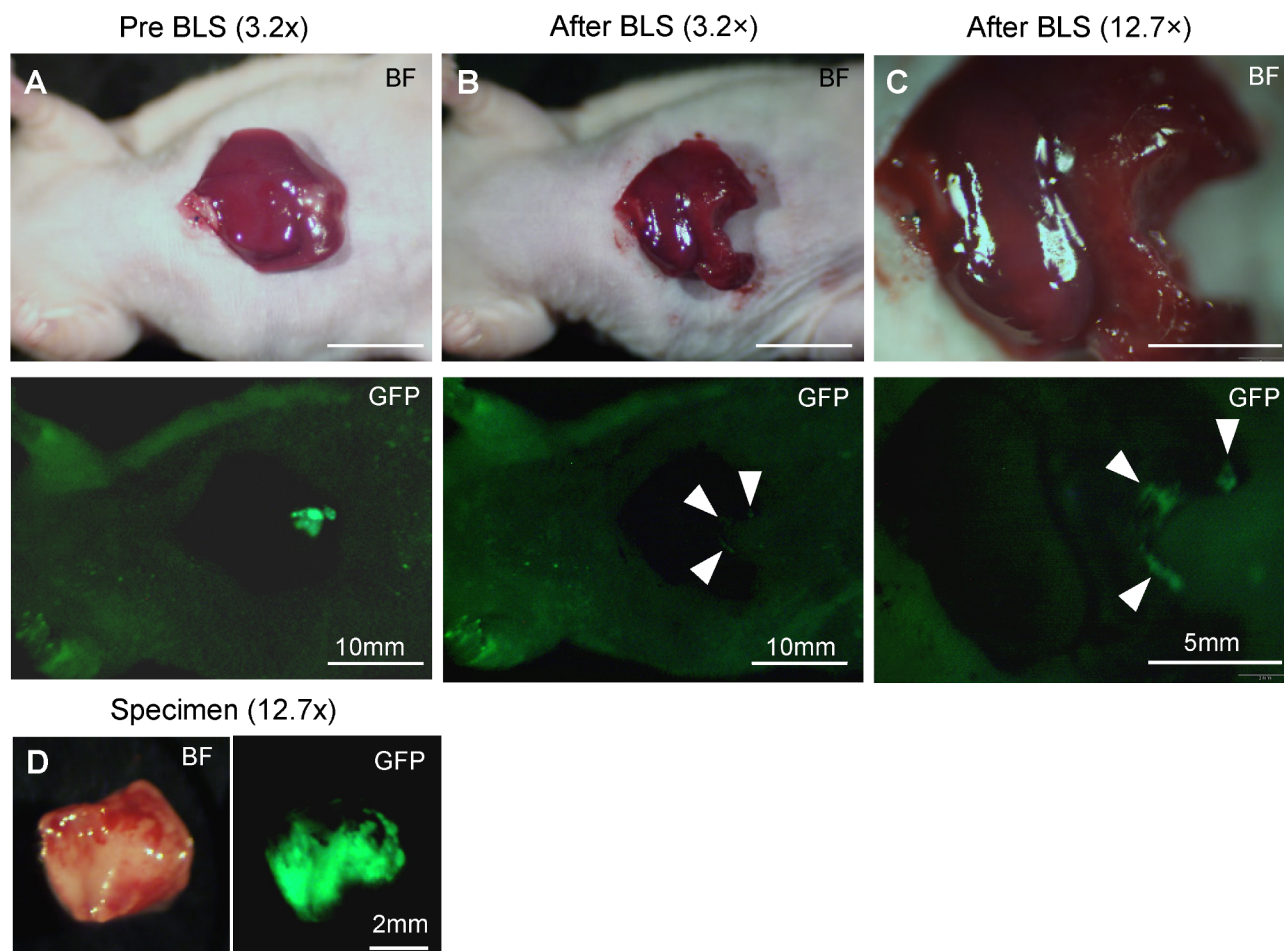


Fig 3. Pre-operative and post-operative images from the orthotopic liver metastasis model treated with BLS. (A)—(C) Upper panels show bright field images, and lower panels are images of tumor fluorescence obtained with the OV100. At low magnification, residual tumor fluorescence was marginally detected. (B) However, at high magnification, residual tumor fluorescence was clearly visualized (arrows) (C). Arrowheads show residual tumor fluorescence in B and C. (D) Resected specimen. Magnifications are indicated above the columns.

doi:10.1371/journal.pone.0138752.g003

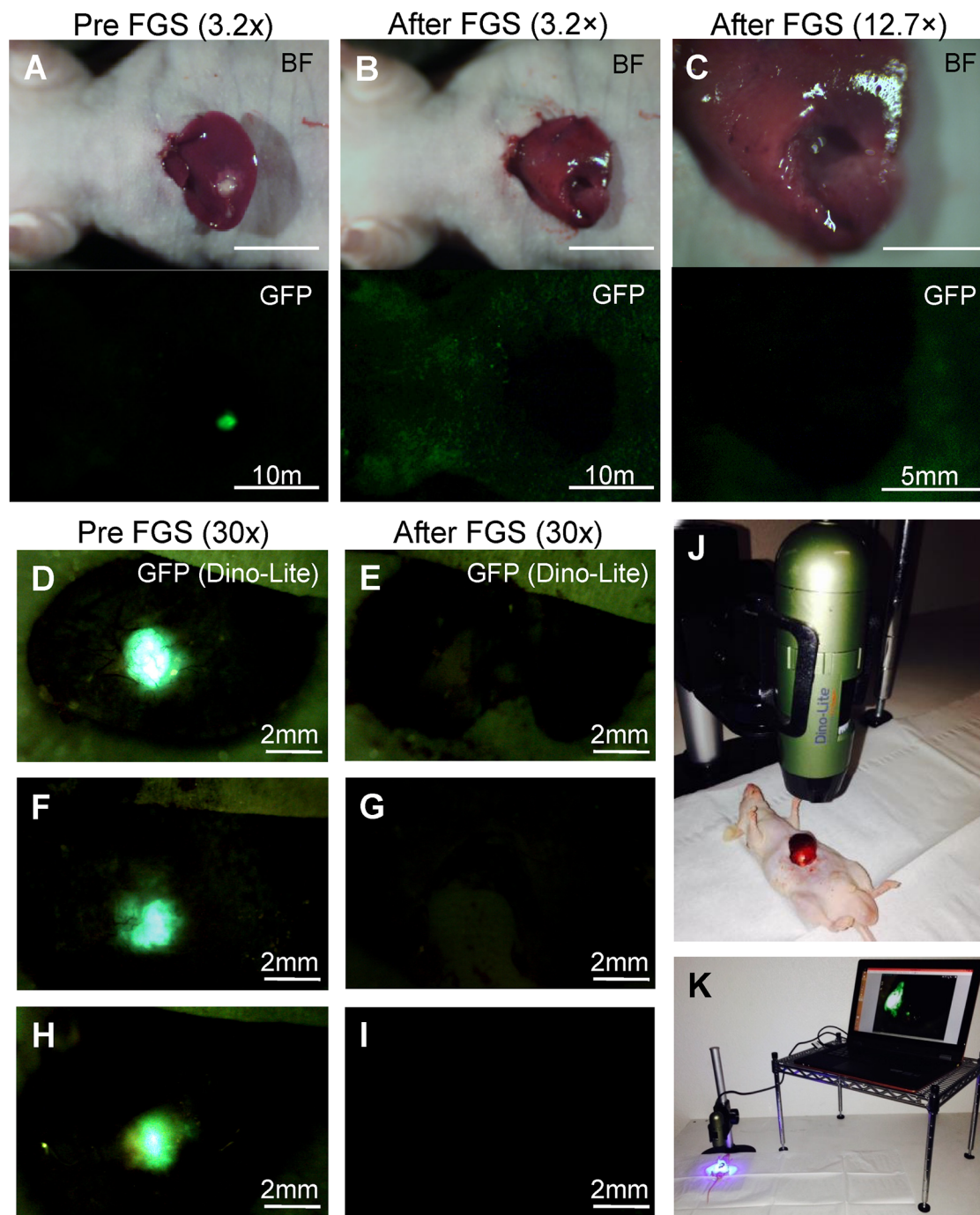


Fig 4. Pre-operative and post-operative images from the orthotopic liver metastasis model treated with FGS. (A)–(C) Upper panels show bright field images, and lower panels are images of tumor fluorescence obtained with the OV100. Residual tumor fluorescence could not be detected even at high magnification (C). (D,F,H) Pre-FGS tumor fluorescence was clearly visualized with the Dino-Lite imaging system. (E,G,I) Dino-Lite imaging showed no evidence of tumor after FGS. (J–K) Dino-Lite settings. (J) After exposing the left lobe of the liver, the mouse was put under the Dino-Lite. (K) Connection between the Dino-Lite and computer. Tumor fluorescence was imaged on the monitor during FGS. Magnifications are indicated above the columns.

doi:10.1371/journal.pone.0138752.g004

variables were determined using the Mann-Whitney U test. A probability value of $P \leq 0.05$ was considered statistically significant.

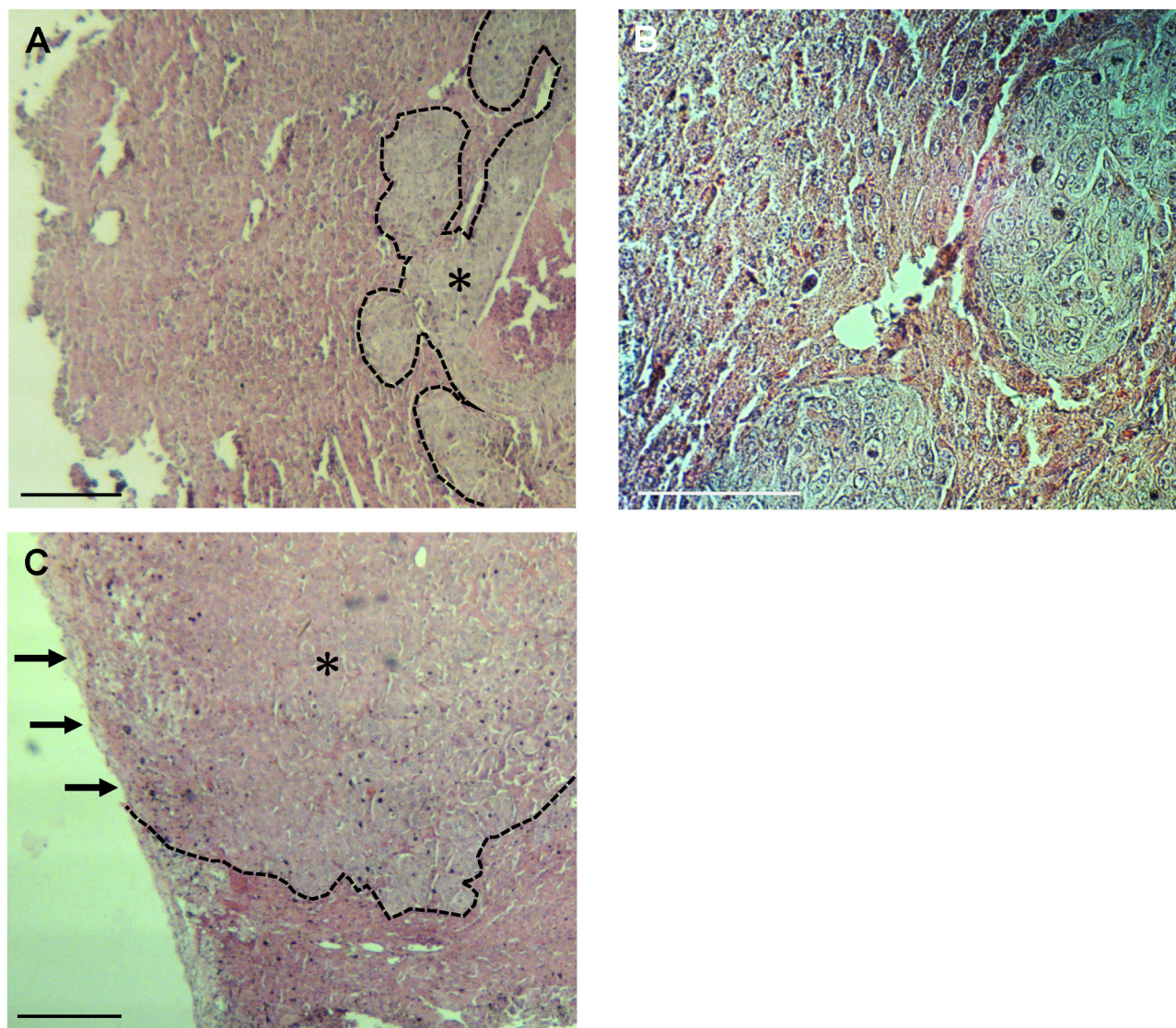


Fig 5. Histological tumor margin of resected specimen. (A)–(C) H&E staining of resected specimen. (A) In the mouse treated with FGS, viable cancer tissue (marked by an asterisk) is surrounded by normal liver tissues. (B) High magnification of (A). (C) In the BLS-treated mouse, viable cancer cells are visible along the resection line. Arrows show residual cancer tissue. Dashed lines separate viable cancer and normal liver tissue. Scale bars: 200 μ m.

doi:10.1371/journal.pone.0138752.g005

Results and Discussion

FGS significantly reduces residual liver metastasis

Single liver metastases were clearly detected preoperatively with the OV100 (Figs 3A and 4A). In the BLS group, residual tumor fluorescence was marginally detected at a magnification of 0.14 \times . However, at a magnification of 0.56 \times , residual cancer was clearly visualized (Fig 3B and 3C). By contrast, residual tumor fluorescence could not be detected even at a magnification of 0.56 \times in the FGS group (Fig 4B and 4C). Tumor fluorescence was also clearly visualized before FGS with the Dino-Lite at a magnification of 30 \times (Fig 4D). Dino-Lite imaging showed no evidence of residual cancer after FGS (Fig 4E). All resected specimens exhibited strong GFP expression (Fig 3D). Histologically, viable cancer was detected on the resection line in the BLS group, but not in the FGS group which had clear margins (Fig 5), which is consistent with the fluorescence data.

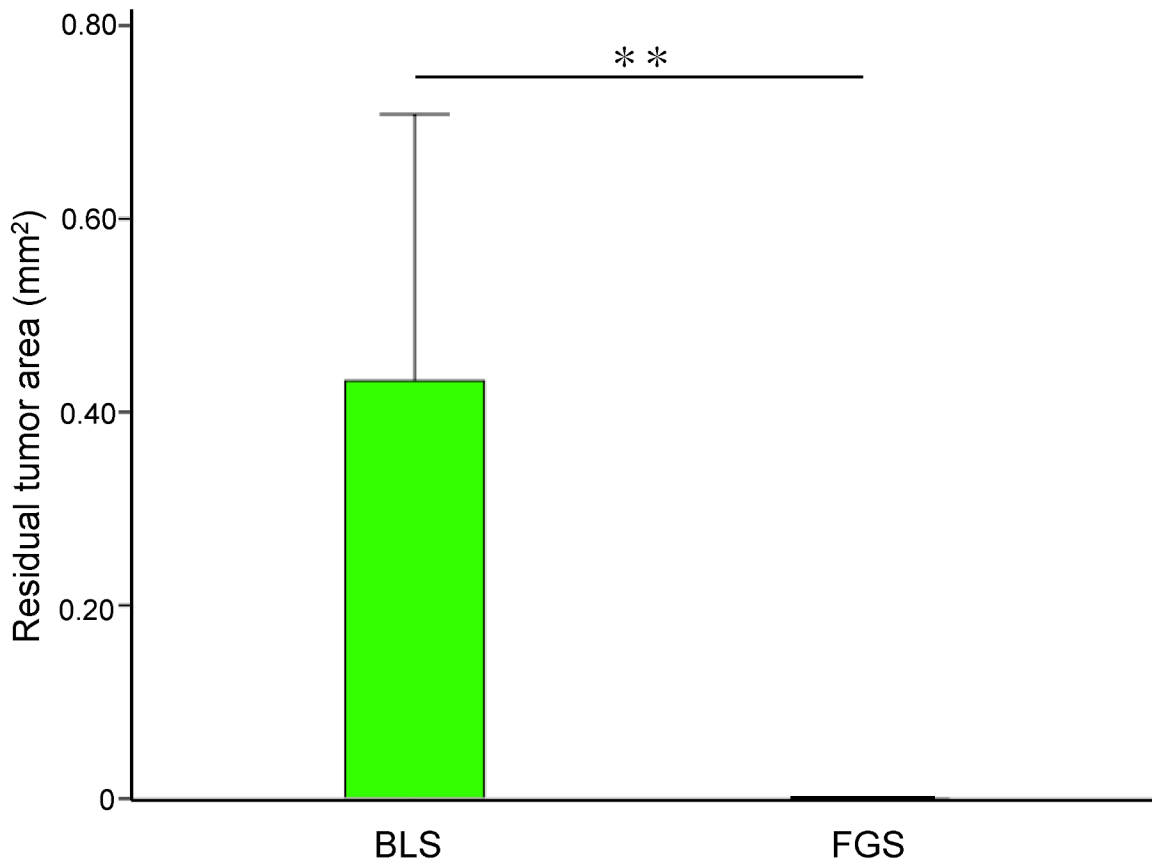


Fig 6. Bar graph of residual tumor area after surgery. No residual tumor was detected in the FGS group. Residual tumor area after BLS was relatively large. Error bar shows SD. ** $P < 0.01$.

doi:10.1371/journal.pone.0138752.g006

Residual tumor area after BLS was significantly larger than after FGS ($0.34 \pm 0.28 \text{ mm}^2$ and 0 mm^2 , respectively; $P = 0.003$; Fig 6).

FGS significantly decreases recurrent tumor area

Laparotomy was performed at 28 postoperative day. Recurrent tumor fluorescence was visualized next to the resected site in the liver in the BLS group, but not in the FGS group (Fig 7). In the FGS group, only autofluorescence was detected.

The FGS procedure for liver metastasis described in the present report had short- and long-term advantages over BLS in that most if not all of the metastasis was resected by FGS compared to BLS (Figs 3–6), and this advantage was maintained even at 28 days post-surgery, where recurrence was greatly reduced by FGS compared to BLS (Fig 7). Future studies will devise curative strategies for FGS of liver metastasis.

Conclusions

The results of present study suggest that FGS has clinical potential of reducing residual cancer in patients who have liver metastasis resected. Clinical application strategies could include labeling the liver metastasis with a tumor-specific monoclonal antibody such as anti-carcinoembryonic antigen (anti-CEA) conjugated to a fluorophore [5–10] or labeled by a telomerase-dependent cancer-specific adenovirus that contains the GFP gene, OBP-401 [11, 12, 17–19].

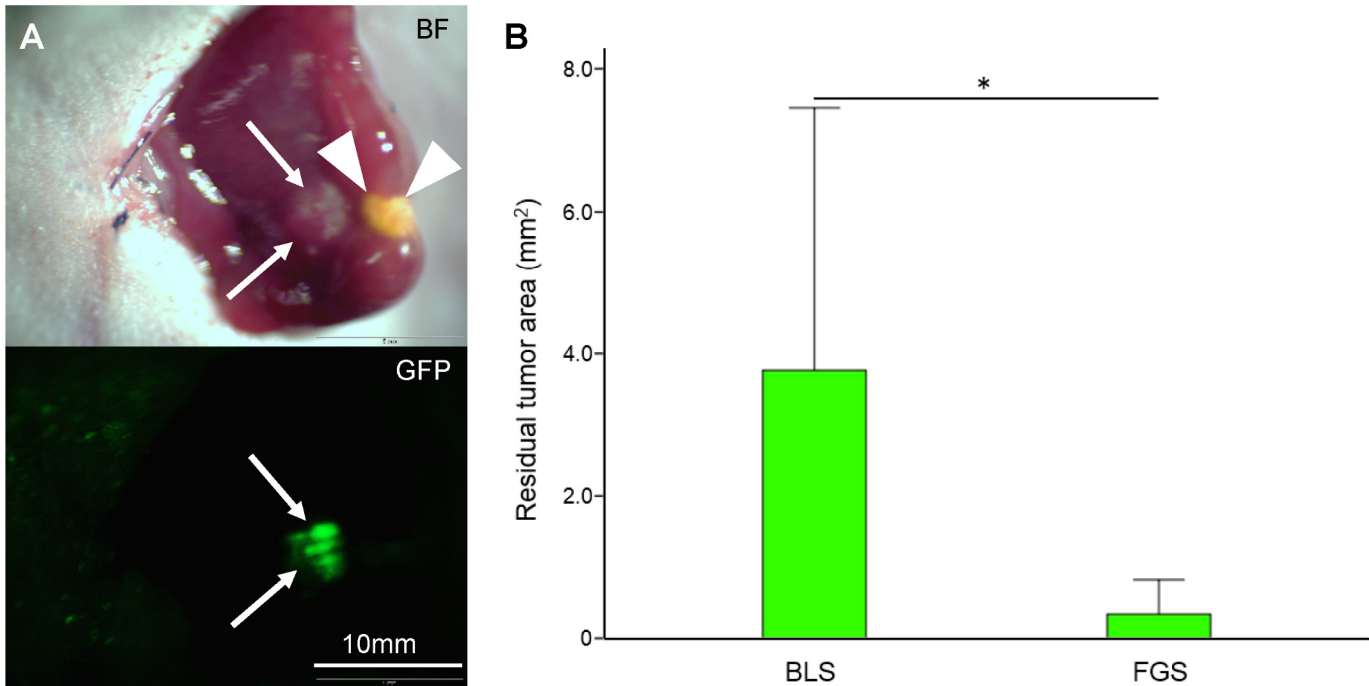


Fig 7. Evaluation of tumor fluorescence at day 28 after surgery. (A) Upper panel shows the bright field image, and lower panel shows the GFP tumor fluorescence image obtained with the OV100 at a magnification of 0.56. Laparotomy was performed at the 28th postoperative day. Bright field image shows tumor in the resection site in the liver (arrows). Strong GFP fluorescence from the tumor is seen in the lower panel. Arrows show recurrent tumor in the resection site. Arrowheads show operative scar on the liver. (B) The GFP tumor fluorescence area was significantly larger in the BLS group compared to the FGS group, where only autofluorescence was detected. Error bars show SD. * $P < 0.05$.

doi:10.1371/journal.pone.0138752.g007

The labeled-antibody strategy is probably feasible in the near future. The viral-labeling strategy will require more safety studies. However, the parent virus of OBP-401, OBP-301, has proven safe in a clinical trial [20]. However, OBP-401 will also have safety tested in a clinical trial.

Supporting Information

S1 ARRIVE Checklist.
(PDF)

Acknowledgments

Dedication

This paper is dedicated to the memory of A. R. Moossa, M.D.

Author Contributions

Conceived and designed the experiments: TM RMH. Performed the experiments: TM YH YZ. Analyzed the data: TM YH YZ TC KT MB IE RMH. Contributed reagents/materials/analysis tools: RMH. Wrote the paper: TM RMH.

References

1. Bouvet M, Hoffman RM (2011) Glowing tumors make for better detection and resection. *Sci Transl Med* 3:110fs10. doi: [10.1126/scitranslmed.3003375](https://doi.org/10.1126/scitranslmed.3003375) PMID: [22116932](https://pubmed.ncbi.nlm.nih.gov/22116932/)

2. Troyan SL, Kianzad V, Gibbs-Strauss SL, Gioux S, Matsui A, Oketokoun R, et al. (2009) The FLARE intraoperative near-infrared fluorescence imaging system: A first-in-human clinical trial in breast cancer sentinel lymph node mapping. *Ann Surg Oncol* 16:2943–2952. doi: [10.1245/s10434-009-0594-2](https://doi.org/10.1245/s10434-009-0594-2) PMID: [19582506](https://pubmed.ncbi.nlm.nih.gov/19582506/)
3. Stummer W, Pichlmeier U, Meinel T, Wiestler OD, Zanella F, Reulen HJ, et al. (2006) Fluorescence-guided surgery with 5-aminolevulinic acid for resection of malignant glioma: A randomised controlled multicentre phase III trial. *Lancet Oncol* 7:392–401. PMID: [16648043](https://pubmed.ncbi.nlm.nih.gov/16648043/)
4. van Dam GM, Themelis G, Crane LM, Harlaar NJ, Pleijhuis RG, Kelder W, et al. (2011) Intraoperative tumor-specific fluorescence imaging in ovarian cancer by folate receptor- α targeting: First inhuman results. *Nat Med* 17:1315–1319. doi: [10.1038/nm.2472](https://doi.org/10.1038/nm.2472) PMID: [21926976](https://pubmed.ncbi.nlm.nih.gov/21926976/)
5. McElroy M, Kaushal S, Luiken G, Moossa AR, Hoffman RM, Bouvet M (2008) Imaging of primary and metastatic pancreatic cancer using a fluorophore-conjugated anti-CA19-9 antibody for surgical navigation. *World J Surg* 32:1057–1066. doi: [10.1007/s00268-007-9452-1](https://doi.org/10.1007/s00268-007-9452-1) PMID: [18264829](https://pubmed.ncbi.nlm.nih.gov/18264829/)
6. Metildi CA, Kaushal S, Snyder CS, Hoffman RM, Bouvet M (2013) Fluorescence-guided surgery of human colon cancer increases complete resection resulting in cures in an orthotopic nude mouse model. *J Surg Res* 179:87–93. doi: [10.1016/j.jss.2012.08.052](https://doi.org/10.1016/j.jss.2012.08.052) PMID: [23079571](https://pubmed.ncbi.nlm.nih.gov/23079571/)
7. Kaushal S, McElroy MK, Luiken GA, Talamini MA, Moossa AR, Hoffman RM, et al. (2008) Fluorophore-conjugated anti-CEA antibody for the intraoperative imaging of pancreatic and colorectal cancer. *J Gastrointest Surg* 12:1938–1950. doi: [10.1007/s11605-008-0581-0](https://doi.org/10.1007/s11605-008-0581-0) PMID: [18665430](https://pubmed.ncbi.nlm.nih.gov/18665430/)
8. Metildi CA, Kaushal S, Luiken GA, Talamini MA, Hoffman RM, Bouvet M. (2014) Fluorescently-labeled chimeric anti-CEA antibody improves detection and resection of human colon cancer in a patient-derived orthotopic xenograft (PDOX) nude mouse model. *J Surg Oncol* 109:451–458. doi: [10.1002/jso.23507](https://doi.org/10.1002/jso.23507) PMID: [24249594](https://pubmed.ncbi.nlm.nih.gov/24249594/)
9. Hiroshima Y, Maawy A, Metildi CA, Zhang Y, Uehara F, Miwa S, et al. (2014) Successful fluorescence-guided surgery on human colon cancer patient-derived orthotopic xenograft mouse models using a fluorophore-conjugated anti-CEA antibody and a portable imaging system. *J Laparoendosc Adv Surg Tech A* 24:241–247. doi: [10.1089/lap.2013.0418](https://doi.org/10.1089/lap.2013.0418) PMID: [24494971](https://pubmed.ncbi.nlm.nih.gov/24494971/)
10. Maawy A, Hiroshima Y, Zhang Y, Luiken GA, Hoffman RM, Bouvet M (2014) Polyethylene glycol (PEG) conjugations of chimeric anti-carcinoembryonic antigen (CEA) labeled with near infrared (NIR) dyes enhances imaging of liver metastases in a nude-mouse model of human colon cancer. *PLoS One* 9: e97965. doi: [10.1371/journal.pone.0097965](https://doi.org/10.1371/journal.pone.0097965) PMID: [24859320](https://pubmed.ncbi.nlm.nih.gov/24859320/)
11. Kishimoto H, Zhao M, Hayashi K, Urata Y, Tanaka N, Fujiwara T, et al. (2009) In vivo internal tumor illumination by telomerase-dependent adenoviral GFP for precise surgical navigation. *Proc Natl Acad Sci USA* 106:14514–14517. doi: [10.1073/pnas.0906388106](https://doi.org/10.1073/pnas.0906388106) PMID: [19706537](https://pubmed.ncbi.nlm.nih.gov/19706537/)
12. Kishimoto H, Aki R, Urata Y, Bouvet M, Momiyama M, Tanaka N, et al. (2011) Tumor-selective adenoviral-mediated GFP genetic labeling of human cancer in the live mouse reports future recurrence after resection. *Cell Cycle* 10:2737–2741. PMID: [21785265](https://pubmed.ncbi.nlm.nih.gov/21785265/)
13. Hoffman RM, Yang M (2006) Subcellular imaging in the live mouse. *Nature Protoc* 1:775–782.
14. Hoffman RM, Yang M (2006) Color-coded fluorescence imaging of tumor-host interactions. *Nature Protoc* 1:928–935.
15. Hoffman RM, Yang M (2006) Whole-body imaging with fluorescent proteins. *Nature Protoc* 1:1429–1438.
16. Yamauchi K, Yang M, Jiang P, Xu M, Yamamoto N, Tsuchiya H, et al. (2006) Development of real-time subcellular dynamic multicolor imaging of cancer-cell trafficking in live mice with a variable-magnification whole-mouse imaging system. *Cancer Res* 66:4208–4214. PMID: [16618743](https://pubmed.ncbi.nlm.nih.gov/16618743/)
17. Yano S, Miwa S, Kishimoto H, Uehara F, Tazawa H, Toneri M, et al. (2015) Targeting tumors with a killer-reporter adenovirus for curative fluorescence-guided surgery of soft-tissue sarcoma. *Oncotarget* 6:13133–13148. PMID: [26033451](https://pubmed.ncbi.nlm.nih.gov/26033451/)
18. Yano S, Miwa S, Kishimoto H, Toneri M, Hiroshima Y, Yamamoto M, et al. (2015) Experimental curative fluorescence-guided surgery of highly invasive glioblastoma multiforme selectively labeled with a killer-reporter adenovirus. *Molecular Therapy* 23:1182–1188. doi: [10.1038/mt.2015.63](https://doi.org/10.1038/mt.2015.63) PMID: [25896244](https://pubmed.ncbi.nlm.nih.gov/25896244/)
19. Yano S, Hiroshima Y, Maawy A, Kishimoto H, Suetsugu A, Miwa S, et al. (2015) Color-coding cancer and stromal cells with genetic reporters in a patient-derived orthotopic xenograft (PDOX) model of pancreatic cancer enhances fluorescence-guided surgery. *Cancer Gene Therapy* 22:344–350. doi: [10.1038/cgt.2015.26](https://doi.org/10.1038/cgt.2015.26) PMID: [26088297](https://pubmed.ncbi.nlm.nih.gov/26088297/)
20. Nemunaitis J, Tong AW, Nemunaitis M, Senzer N, Phadke AP, Bedell C, et al. (2010). A phase I study of telomerase-specific replication competent oncolytic adenovirus (telomelysin) for various solid tumors. *Mol Ther* 18:429–434. doi: [10.1038/mt.2009.262](https://doi.org/10.1038/mt.2009.262) PMID: [19935775](https://pubmed.ncbi.nlm.nih.gov/19935775/)